

Prostate Cancer Detection in Patients With Total Serum Prostate-Specific Antigen Levels of 4–10 ng/mL: Diagnostic Efficacy of Diffusion-Weighted Imaging, Dynamic Contrast-Enhanced MRI, and T2-Weighted Imaging

Tsutomu Tamada¹
Teruki Sone¹
Hiroki Higashi¹
Yoshimasa Jo²
Akira Yamamoto¹
Akihiko Kanki¹
Katsuyoshi Ito¹

OBJECTIVE. The purpose of this study is to evaluate the utility of T2-weighted imaging, dynamic contrast-enhanced MRI (DCE-MRI), and diffusion-weighted imaging (DWI) for detecting prostate cancer in patients with total serum prostate-specific antigen (PSA) levels of 4–10 ng/mL, which is referred to as the “gray zone.”

MATERIALS AND METHODS. Fifty patients with gray-zone PSA levels underwent MRI before biopsy. According to the sites of biopsy, the prostate was divided into eight regions on MRI scans. These regions were evaluated individually for the following features: detectability of prostate cancer on per-region and per-patient bases, and relationship between tumor size and positive or negative MRI findings for tumor detection.

RESULTS. On a per-region basis, the sensitivity and specificity of tumor detection were 36% and 97% for T2-weighted imaging, 43% and 95% for DCE-MRI, 38% and 96% for DWI, and 53% and 93% for the combined method of MRI, respectively. The sensitivity of combined MRI to detect tumor was significantly higher than those of the individual methods ($p < 0.001$ to $p = 0.001$). Tumor size was significantly larger in regions with positive MRI findings than in regions with negative MRI findings ($p = 0.004$). On a per-patient basis, sensitivity and specificity of combined MRI to detect prostate cancer were 83% and 80%, respectively.

CONCLUSION. Combined T2-weighted imaging, DWI, and DCE-MRI findings appear to be potentially useful for detecting and managing prostate cancer, even when performed for patients with gray-zone PSA levels.

Keywords: cancer screening, early diagnosis of cancer, MRI, prostate-specific antigen, prostatic neoplasms

DOI:10.2214/AJR.10.5923

Received October 9, 2010; accepted after revision January 28, 2011.

This study was supported by a Japan Society for the Promotion of Science Grant-in-Aid for Scientific Research (grant 21591582).

¹Department of Radiology, Kawasaki Medical School, 577 Matsushima, Kurashiki City, Okayama 701-0192, Japan. Address correspondence to T. Tamada (ttamada@med.kawasaki-m.ac.jp).

²Department of Urology, Kawasaki Medical School, Kurashiki City, Okayama, Japan.

AJR 2011; 197:664–670

0361–803X/11/1973–664

© American Roentgen Ray Society

More than 190,000 men in the United States received a diagnosis of prostate cancer in 2009, and the disease is the second leading cause of cancer deaths among men [1]. In Japan, which has the second highest life expectancy (78.64 years) in the world, the growing elderly population has led to a sharp increase in the number of prostate cancer cases among elderly men, and prostate cancer is now expected to show the highest increase in mortality rate compared with other common cancers, such as stomach and lung cancer [2–5].

Early diagnosis of prostate cancer is essential to reduce mortality rates. The serum prostate-specific antigen (PSA) test offers one of the best tests for early detection of prostate cancer [6, 7]. This noninvasive test is thus currently in wide use as a method of screening for prostate cancer, particularly in the elderly male population [8]. However, although PSA level has high sensitivity for prostate cancer detection, its specificity is insufficient when PSA levels are rela-

tively low, such as within the so-called “gray zone” of 4–10 ng/mL [9]. The positive predictive value (PPV) of PSA for prostate cancer detection using transrectal ultrasound (TRUS)-guided biopsy or radical retropubic prostatectomy is estimated to be 30–42% in patients with gray-zone PSA levels [10–12]. This is because, apart from prostate cancer, several noncancerous causes, such as benign prostatic hyperplasia and chronic prostatitis, can increase PSA levels [13]. Accordingly, about 70% of men with gray-zone PSA levels may undergo unnecessary biopsy [14]. Accurate detection of prostate cancer thus has the potential for decreasing unnecessary biopsies. So far, only a few studies using T2-weighted imaging or MR spectroscopic imaging (MRSI) have shown their potential in detecting prostate cancer in patients with gray-zone PSA levels [15–17].

The utility of combined MRI using T2-weighted imaging, dynamic contrast-enhanced MRI (DCE-MRI), diffusion-weighted imaging (DWI) with apparent diffusion

Diagnostic Efficacy of Combined MRI in Detecting Prostate Cancer

coefficient (ADC), and MRSI in the diagnosis of localized prostate cancer arising not only in the peripheral zone (PZ) but also in the transition zone (TZ) has been clarified in recent years in a number of clinical studies [18–25]. In the studies that included patients with higher PSA levels (> 10 ng/mL), sensitivity, specificity, accuracy, PPV, and negative predictive value (NPV) for the detection of prostate cancer using combined MRI were 69–95%, 63–96%, 68–92%, 75–86%, and 80–95%, respectively [18–20, 23–25]. However, to our knowledge, no studies with multiparametric MRI focusing on the detection of prostate cancer in men with gray-zone PSA levels have been reported.

The aim of this study was to evaluate the utility of T2-weighted MRI, DCE-MRI, and DWI for the detection of prostate cancer in patients with total serum PSA levels of 4–10 ng/mL.

Materials and Methods

Patient Characteristics

This retrospective study was approved by the institutional review board, and the need for informed consent from patients was waived.

A total of 54 men with gray-zone PSA levels underwent MRI of the prostate within 3 months before TRUS-guided biopsy between January 2006 and December 2009 in our institution. Four patients were excluded because of incomplete MRI examination ($n = 2$) or cryptogenic intraprostatic hemorrhage ($n = 2$). Thus, 50 men (mean age, 70 years; range, 40–84 years) were included in this study. Mean PSA level was 6.84 ng/mL (median,

6.68 ng/mL; range, 4.06–9.94 ng/mL). The mean interval between biopsy and MRI was 23 days (range, 1–87 days). None of the patients was diagnosed with prostate cancer before MRI.

A total of 12 specimens (eight from the PZ and four from the TZ) were taken from each patient during TRUS-guided systematic prostate biopsy by an urologist with 15 years of experience in prostate biopsy.

MRI

After intramuscular administration of glucagon to decrease intestinal peristalsis, prostate MRI was performed in all patients under fasting conditions. MRI was performed with a 1.5-T MRI scanner (Signa Excite High speed, GE Healthcare) with a maximum gradient amplitude of 33 mT/m and a maximum slew rate of 77 mT/m/s. A body coil was used for signal excitation, with a multichannel phased-array torso coil (catalog no. S75292E, GE Healthcare) for signal reception.

MRI protocols included axial and coronal T2-weighted fast spin-echo (FSE) imaging, axial T2-weighted echo-planar imaging (EPI), axial DWI, axial DCE-MRI, and axial unenhanced and contrast-enhanced T1-weighted FSE imaging. Axial DWI was performed using a multisection spin-echo single-shot EPI sequence. ADC maps were reconstructed by calculating the ADC in each pixel of each slice. DCE-MRI was performed using an FSE sequence or a 3D T1-weighted gradient-echo liver acquisition with volume acceleration (LAVA) sequence. Data acquisition for DCE-MRI began simultaneously with initiation of IV injection of gadopentetate dimeglumine (Magnevist, Bayer Schering Pharma) at 0.1 mmol/kg body

weight at a rate of 3 mL/s via a power injector (Sonic Shot 50, Nemoto Kyorindo), followed by a 40-mL saline flush at 3 mL/s as a gadopentetate dimeglumine injection. Multiphase DCE images were obtained every 30 seconds for 150 seconds in an FSE sequence (six phases) or every 20 seconds for 120 seconds in a LAVA sequence (seven phases) without breath-holding by patients.

The acquisition parameters for the MRI pulse sequences are listed in Table 1.

Image Interpretation and Data Analysis

Two radiologists with 11 and 7 years of experience in prostate MRI conducted a consensus review of MRI examinations for the 50 patients. The reviewers were aware that patients had been referred for MRI on suspicion of prostate cancer with PSA levels of 4–10 ng/mL but were blinded to all other clinical and histopathologic findings. Furthermore, the reviewers were blinded to the findings of the other sequences at the time of review.

Intraprostatic hemorrhage was considered to be present when an area of signal hyperintensity was identified within the prostate gland on T1-weighted imaging. Two patients who were diagnosed with intraprostatic hemorrhage on T1-weighted imaging were excluded from this study because of the limited accuracy caused by bleeding for tumor localization of prostate cancer on MRI.

According to the sites of biopsy, the prostate gland was divided into eight regions on MRI scans [19, 26] (Fig. 1). To distinguish PZ and TZ, reviewers mainly used T2-weighted MRI scans, because zonal anatomy of the prostate can be seen only on these images [27]. Landmarks used to distinguish PZ and TZ were the urethra, capsule

TABLE 1: MRI Parameters Used in the Current Study

Parameter	Sequence					
	T1-Weighted FSE	T2-Weighted FSE	T2-Weighted EPI	DWI (Single-Shot EPI)	DCE-MRI (FSE)	DCE-MRI (LAVA)
TR (ms)	425	3600	2500	5000	350	4.7
TE (ms)	9.3	102	80	63.8	9	2.2
Bandwidth (kHz)	31.2	20.8	250	250 ^a	31.2	62.5
Echo-train length	2	16	NA	NA	3	NA
Matrix size	320 × 256	320 × 320	256 × 256	128 × 192	256 × 128	288 × 192
FOV (cm)	24 × 24	24 × 24	24 × 24	36 × 36	27 × 27	35 × 35
No. of acquisitions	3	4	8	8	1	0.78
Slice thickness (mm)	5	4	5	5	5	3
Interslice gap (mm)	1	0.5	1	1	2.5	0
Parallel imaging factor	NA	NA	NA	2	NA	2
Scan time	2 min 42 s	4 min 47 s	2 min 43 s	2 min 40 s	3 min (30 s × 6 phases)	2 min 20 s (20 s × 7 phases)

Note—Diffusion-weighted imaging (DWI) was performed with motion-probing gradient pulses applied sequentially along three orthogonal orientations with two b factors (0 and 800 s/mm²). DCE-MRI = dynamic contrast-enhanced MRI, EPI = echo-planar imaging, FSE = fast spin-echo, LAVA = liver acquisition with volume acceleration, NA = not applicable.

^aFrequency-encoding direction.

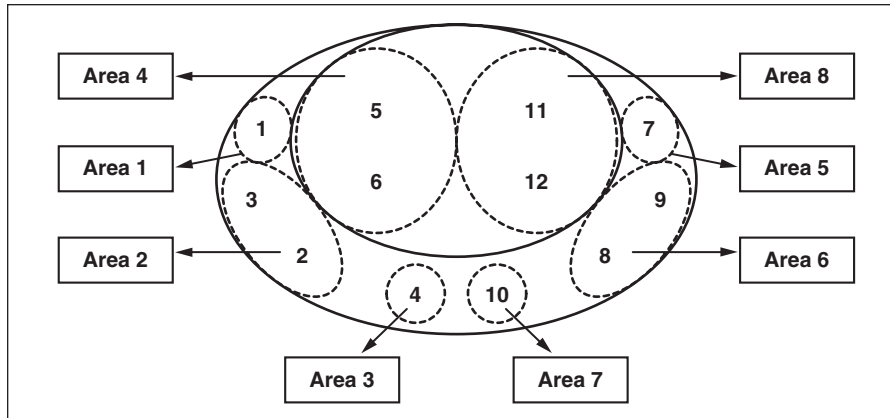


Fig. 1—Schematic illustration showing 12 sites of core needle biopsy in eight areas of prostate on MRI scans. According to sites of biopsy (1–12), prostate gland was divided into eight areas on MRI scans. That is, base right in peripheral zone (PZ) (1), middle right and far lateral right in PZ (2 and 3), apex right in PZ (4), ventral and dorsal right in transition zone (TZ) (5 and 6), base left in PZ (7), middle left and far lateral left in PZ (8 and 9), apex left in PZ (10), and ventral and dorsal left in TZ (11 and 12) as biopsy sites were designated as base right (Area 1), middle right (Area 2), apex right (Area 3), TZ right (Area 4), base left (Area 5), middle left (Area 6), apex left (Area 7), and TZ left (Area 8), respectively. (Reprinted with permission from [19])

of the prostate gland, and the surgical pseudocapsule. In the PZ, sections through the bladder neck and proximal prostatic urethra were considered as the base, whereas the prostatic apex was defined by the doughnut-shaped appearance of the distal prostatic urethra. The remainder of the PZ was considered as the middle [28]. These regions were evaluated individually with regard to the detectability of prostate cancer. Prostate cancer was localized independently on each MRI study according to standard criteria. On MRI scans, lesions fulfilling the following criteria were regarded as prostate cancer: first, on T2-weighted imaging (FSE or EPI or both), a circumscribed round or triangular-shaped area in the PZ with homogeneous signal hypointensity and mass effect [29] or an area in the TZ with homogeneous signal hypointensity, ill-defined margins, and lack of capsule [27]; second,

on DWI and ADC maps, an area with focal signal hyperintensity on DWI and with focal signal hypointensity on the ADC map relative to background prostatic parenchyma; or finally, on DCE-MRI, an area with focal early enhancement until the third phase in the FSE sequence or the fourth phase in the LAVA sequence (60 seconds after administration of contrast medium). In the interpretation of images from DWI and DCE-MRI, we referred to T2-weighted imaging, to confirm anatomic positions after the assessment of each image.

The tumor site on each MRI scan was considered to match histologic findings if the tumor depicted on the image was present in the same region of the prostate indicated in the pathology report for the TRUS-guided biopsy specimen. First, on a per-region basis, diagnostic sensitivity, specificity, accuracy, PPV, and NPV were calculated for

T2-weighted imaging, DWI, DCE-MRI, and the combination of all three MRI techniques (combined MRI). In combined MRI, when a positive finding according to the criteria mentioned previously was recognized for at least one of the three methods in each region for each patient, the region was considered to contain prostate cancer. Next, on a per-patient basis, diagnostic sensitivity, specificity, accuracy, PPV, and NPV were calculated for T2-weighted imaging, DWI, DCE-MRI, and combined MRI. On a per-patient basis, when each MRI technique and combined MRI showed a positive finding for at least one of the eight regions, that patient was considered to have prostate cancer.

In addition, reviewers also recorded the tumor volume and Gleason score of prostate cancer in positive biopsy sites from the pathology report for the TRUS-guided biopsy specimen after the MRI interpretation. An index of tumor size was calculated using the total cancer length within each biopsy specimen instead of tumor volume [19].

Statistical Analysis

Differences in sensitivity, specificity, PPV, and NPV between any two MRI methods were tested using the McNemar test. The Mann-Whitney U test was used to determine significant differences in indexes of tumor size and Gleason score for pathologically diagnosed prostate cancer between regions of positive and negative MRI findings. Statistical analyses were performed using SPSS software (version 17.0, SPSS). All statistical tests were two sided, and *p* values of 0.05 or less were considered indicative of a significant difference.

Results

Prostate Biopsy Results

TRUS-guided prostate biopsy revealed prostate cancer in 35 of 50 patients (70%) and in

TABLE 2: Detection of Prostate Cancer Using Various MRI Methods in 50 Patients With Gray-Zone Prostate-Specific Antigen Levels

MRI Method	Sensitivity	Specificity	Accuracy	PPV	NPV
Per-region basis (n = 400)					
T2-weighted imaging	36 (37/103)	97 (289/297)	82 (326/400)	82 (37/45)	81 (289/355)
DWI	38 (39/103)	96 (286/297)	81 (325/400)	78 (39/50)	82 (286/350)
DCE-MRI	43 (44/103)	95 (282/297)	82 (326/400)	75 (44/59)	83 (282/341)
Combined MRI ^a	53 (55/103)	93 (277/297)	83 (332/400)	73 (55/75)	85 (277/325)
Per-patient basis (n = 50)					
T2-weighted imaging	60 (21/35)	87 (13/15)	68 (34/50)	91 (21/23)	48 (13/27)
DWI	69 (24/35)	87 (13/15)	74 (37/50)	92 (24/26)	54 (13/24)
DCE-MRI	74 (26/35)	80 (12/15)	76 (38/50)	90 (26/29)	57 (12/21)
Combined MRI ^a	83 (29/35)	80 (12/15)	82 (41/50)	91 (29/32)	67 (12/18)

Note—Data are percentages, with values used to calculate these percentages provided in parentheses. DCE-MRI = dynamic contrast-enhanced MRI, DWI = diffusion-weighted imaging, NPV = negative predictive value, PPV = positive predictive value.

^aCombined MRI refers to combined use of T2-weighted imaging, DWI, and DCE-MRI.

Diagnostic Efficacy of Combined MRI in Detecting Prostate Cancer

103 of 400 regions (26%). Among the 103 positive regions, 74 (72%) were located in the PZ and the rest were in the TZ. PZ lesions consisted of 19 in the base, 33 in the middle, and 22 in the apex. The median Gleason tumor score was 7 (range, 6–10), and the mean index for tumor size was 0.31 (range, 0.06–0.94).

Detection of Prostate Cancer

Sensitivity, specificity, accuracy, PPV, and NPV on both a per-region basis and a per-patient basis are shown in Table 2. On a per-region basis, the sensitivity of combined MRI to detect tumor was higher than those for T2-weighted imaging, DWI, and DCE-MRI individually (53% vs 36–43%), although specificity was slightly decreased (93% vs 95–97%). Sensitivity differed significantly between T2-weighted imaging and combined MRI ($p < 0.001$), between DWI and combined MRI ($p < 0.001$), and between DCE-MRI and combined MRI ($p = 0.001$). Specificity differed significantly between T2-weighted imaging and combined MRI ($p < 0.001$), between DWI and combined MRI ($p = 0.004$), and between DCE-MRI and combining MRI ($p = 0.031$). No significant differences were observed for any other pairwise comparisons.

On a per-patient basis, sensitivity, specificity, accuracy, PPV, and NPV of combined MRI to detect prostate cancer were 83%, 80%, 82%, 91%, and 67%, respectively, showing the increase of sensitivity and PPV and the decrease of specificity and NPV compared with those on a per-region basis. The sensitivity of combined MRI to detect tumor was higher than those for T2-weighted imaging, DWI, and DCE-MRI individually (83% vs 60–74%), although specificity was equivalent or slightly decreased (80% vs 80–87%). Sensitivity differed significantly between T2-weighted imaging and combined MRI ($p = 0.008$). No significant differences were observed for any other pairwise comparisons.

Comparison of Tumor Size and Gleason Score Between Regions of Positive and Negative MRI Findings of Prostate Cancer

The index of tumor size was significantly larger in regions of positive MRI findings (0.36 ± 0.20) than in regions of negative MRI findings (0.25 ± 0.19 ; $p = 0.004$). Actually, the mean total cancer length in regions of positive and negative MRI findings was 6.7 mm and 3.6 mm, respectively. Conversely, the Gleason score for regions of positive MRI findings (7.17 ± 0.83) was comparable

to that for regions of negative MRI findings (7.45 ± 1.34), with no significant difference.

Tumor Detection by Three MRI Methods in Prostate Cancer With Positive MRI Findings

Positive MRI findings were seen in 55 of 103 regions (53%). These lesions could be diagnosed only on T2-weighted imaging in five regions, only by DWI in two regions, only by DCE-MRI in nine regions, by both T2-weighted imaging and DWI in four regions, by both T2-weighted imaging and DCE-MRI in two regions, by both DWI and

DCE-MRI in seven regions, and by all three methods in 26 regions (Figs. 2–4).

Discussion

Our region-based analysis using 1.5-T prostate MRI for the detection of prostate cancer in patients with gray-zone PSA levels showed that sensitivity was low (36–53%), specificity was very high (93–97%), and accuracy, PPV, and NPV were moderately high (81–83%, 73–82%, and 81–85%, respectively). Sensitivity was significantly higher for combined MRI (53%) than for T2-weighted imaging, DCE-

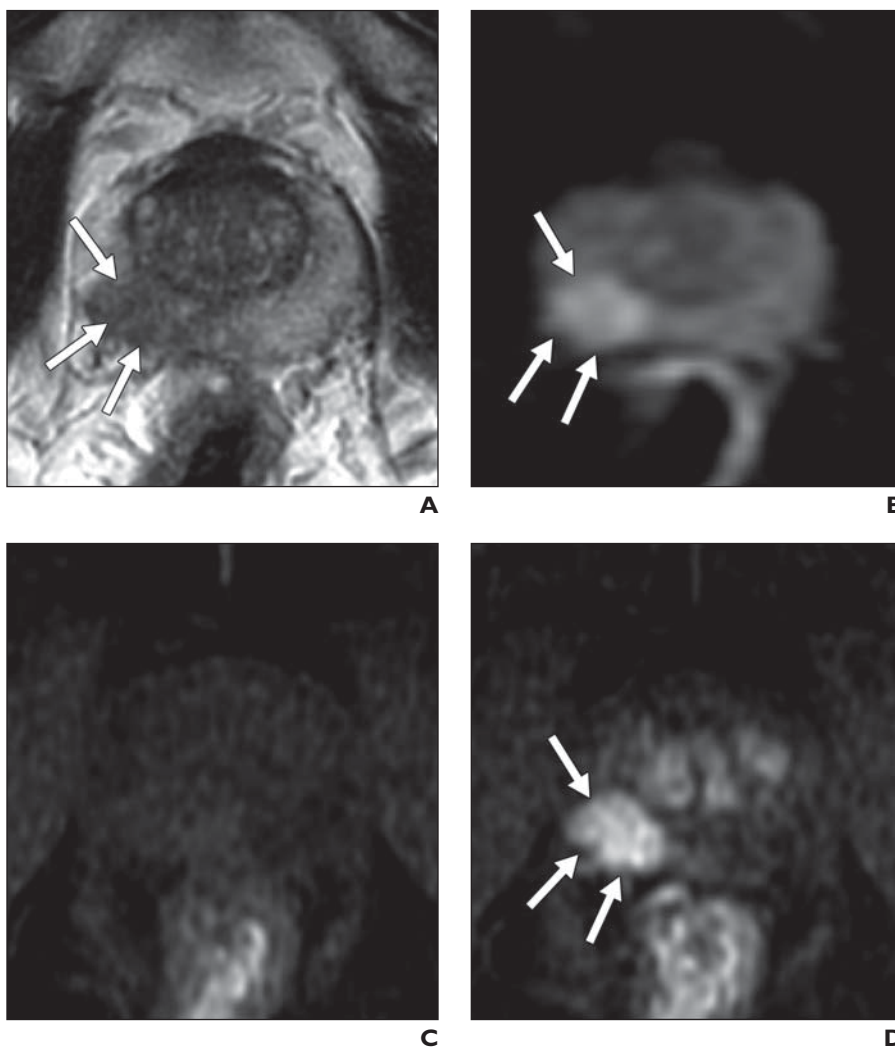


Fig. 2—72-year-old man with prostate-specific antigen level of 4.22 ng/mL and positive results of transrectal biopsy. Transverse MRI of prostate indicated Gleason score of 9 in middle right and transition zone (TZ) right regions. **A**, T2-weighted fast spin-echo image (3600/102) shows peripheral zone (PZ) cancer (arrows) in middle right region as homogeneous hypointense lesion with mass effect. **B**, Diffusion-weighted image shows PZ cancer (arrows) as focal hyperintensity. **C** and **D**, PZ cancer is seen as focal early enhancement on dynamic contrast-enhanced MRI using liver acquisition with volume acceleration sequence in first (unenhanced; **C**) and fourth (arrows, **D**) phases. Cancer lesion in TZ right region could not be detected by any of three MRI techniques.

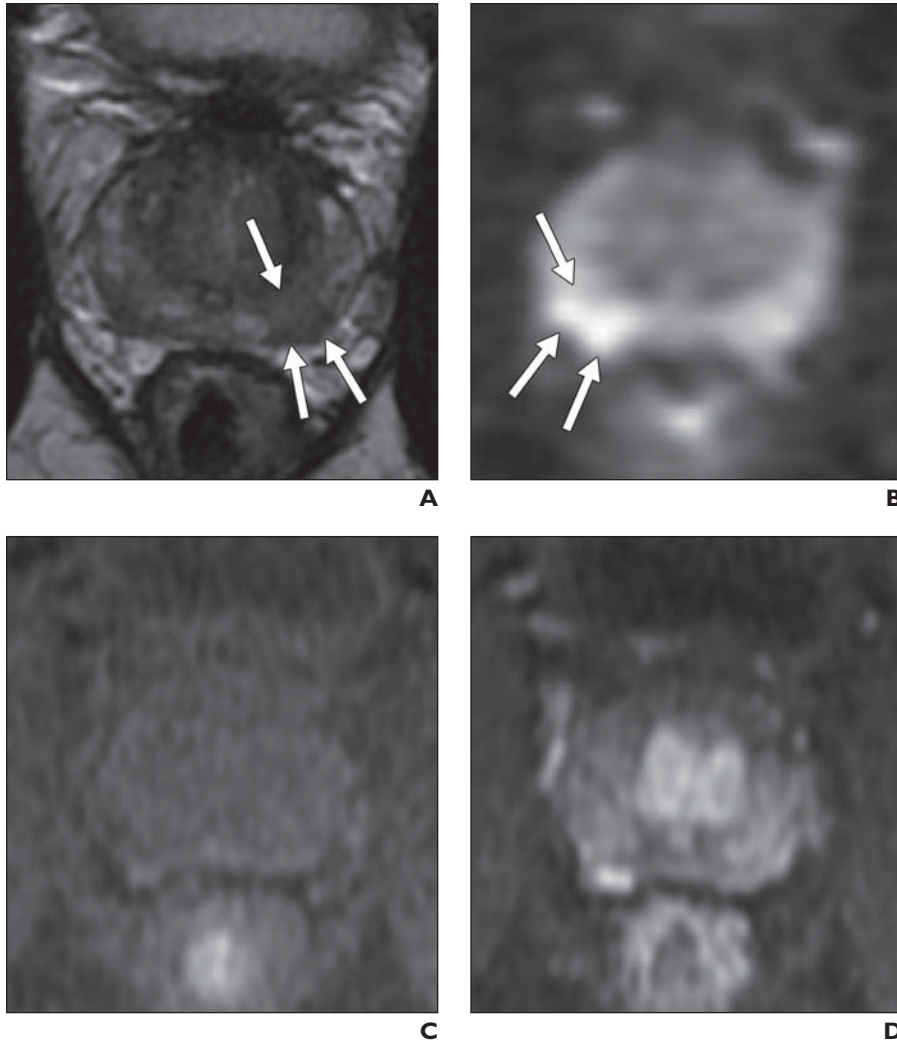


Fig. 3—67-year-old man with PSA level of 8.34 ng/mL and positive results of transrectal biopsy. Transverse MRI of prostate indicated Gleason score of 7 in middle right, apex right, transition zone (TZ) right, base left, middle left, apex left, and TZ left regions.

A, T2-weighted fast spin-echo (FSE) image (3600/102) shows peripheral zone (PZ) cancer (arrows) as homogeneous signal hypointense lesion with mass effect in middle left region of PZ.

B, Diffusion-weighted image shows PZ cancer (arrows) as focal signal hyperintensity in middle right region of PZ.

C and D, No areas of focal early enhancement representing prostate cancer were observed on dynamic contrast-enhanced MRI using FSE sequences of first (unenhanced; **C**) and third (**D**) phases. Left middle cancer could thus be detected only by T2-weighted imaging, whereas right middle cancer could be detected only by diffusion-weighted imaging.

MRI, or DWI individually, although it was not high enough to be used as a screening or detection tool in this subset of patients. Sensitivity for combined MRI in this study was lower than that in recent reports (69–88%), whereas specificity, accuracy, PPV, and NPV were almost equivalent [18, 19, 23, 25]. This difference could be attributable to a difference in PSA levels of patients, because these previous studies included patients with PSA levels not only in the gray zone but also those with PSA levels higher than 10 ng/mL.

Several factors can be considered contributory to the decreased sensitivity for prostate cancer detection in patients with gray-zone PSA levels. First, in our results, tumor size rather than Gleason tumor score showed a significant difference between regions of positive and negative MRI findings. Because spatial resolution would be a limiting factor for imaging small tumors, higher resolution may increase the sensitivity, especially in the low-resolution study such as DWI. Second, a recent study of 18 patients with almost gray-

zone PSA levels (range, 2.27–10.99 ng/mL; median, 4.59 ng/mL) reported that the degree of intermixed normal tissue within the prostate cancer affects ADC values and T2 properties [30]. That is, although ADC values and T2 signal intensities are low in dense prostate tumors, they resemble those of normal prostatic tissue in sparse tumors [30]. Furthermore, among the 55 lesions with positive MRI findings in the present study, 16 (29%) were diagnosed by only one of the three MRI methods of T2-weighted imaging, DCE-MRI, and DWI. This finding suggests that the contribution of tissue characteristics such as morphologic changes on T2-weighted MRI, tumor vascularity on DCE-MRI, and water diffusion showing the degree of cellular density on DWI varies among prostate tumors in patients with gray-zone PSA levels [31]. Therefore, in prostate cancer with gray-zone PSA levels, both tumor size and tissue heterogeneity may limit the detectability of tumor by combined MRI using T2-weighted imaging, DWI, and DCE-MRI.

The decrease in detectability induced by such unfavorable factors may be overcome by using an endorectal coil to provide a substantial increase in the signal-to-noise ratio [32] or by the addition of MRSI to provide metabolic information about prostate tissue [15, 31, 33]. However, these techniques are disadvantaged by the discomfort associated with coil insertion, long acquisition time, and possible variability in results depending on shimming or postprocessing [18, 31] and may thus be unsuitable for daily clinical use in the detection of prostate cancer. A recent prospective study with 3-T MRI comparing a body-array coil and an endorectal coil reported that T2-weighted MRI with an endorectal coil had significantly higher image quality and tumor detectability in comparison with a body-array coil [34]. On the other hand, the ranges of ADC values of prostate cancer obtained using 1.5-T MRI (600–1000 s/mm²) were almost equivalent whether an endorectal coil (0.96–1.45 × 10⁻³ mm²/s) [21, 35, 36] or body-array coil (0.93–1.21 × 10⁻³ mm²/s) was used [18, 37, 38].

Compared with region-based analysis, patient-based analysis showed increased sensitivity (60–83%) and PPV (90–92%), almost equivalent accuracy (68–82%), and decreased specificity (80–87%) and NPV (48–67%). In particular, both the high sensitivity and the moderate NPV on combined MRI will help urologists to decide whether to perform prostate biopsy or follow up using PSA in patients with gray-zone PSA levels.

Diagnostic Efficacy of Combined MRI in Detecting Prostate Cancer

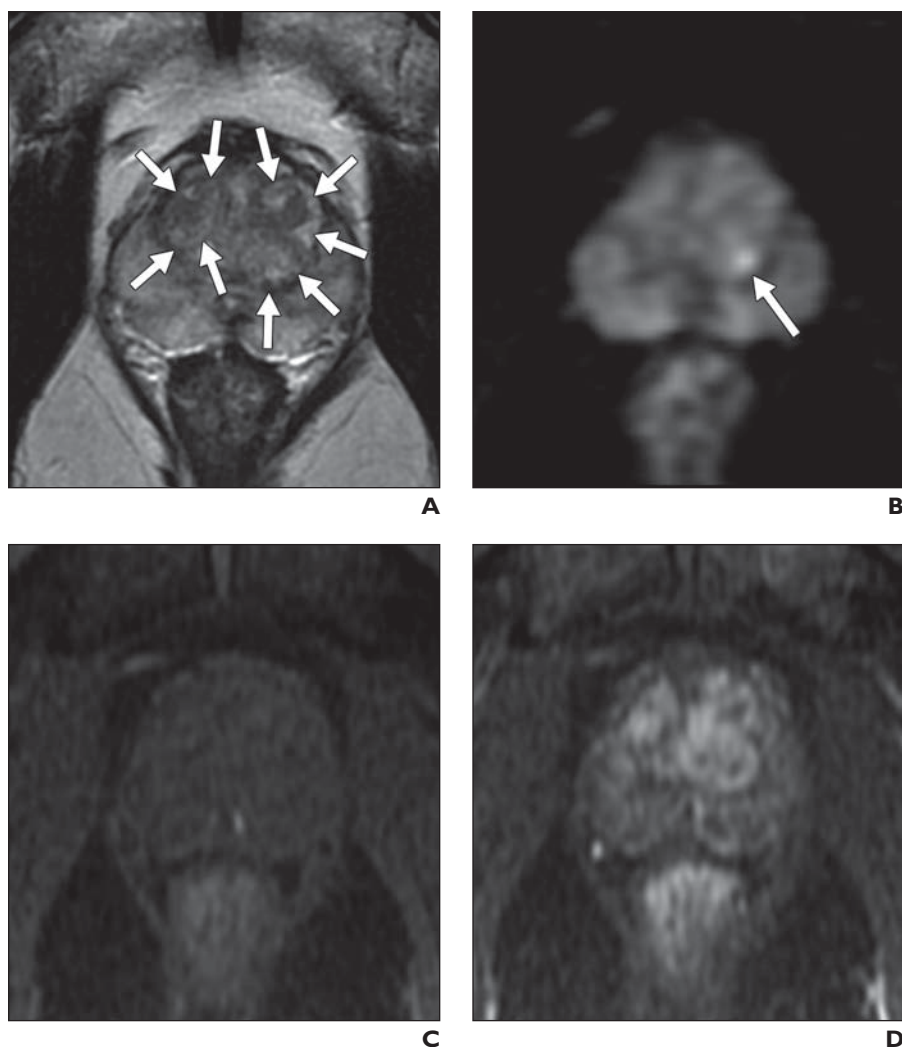


Fig. 4—72-year-old man with PSA level of 8.07 ng/mL and positive results of transrectal biopsy. Transverse MRI of prostate indicated Gleason score of 6 in transition zone (TZ) left region.

A, T2-weighted fast spin-echo (FSE) image (3600/102) shows benign hyperplastic nodules (arrows) as heterogeneous hypointense lesions with hyperintense spots in TZ right and TZ left regions.
B, Diffusion-weighted image shows TZ cancer (arrow) as focal signal hyperintensity in TZ left region.
C and **D**, No areas of focal early enhancement suggestive of prostate cancer were observed on dynamic contrast-enhanced MRI using FSE sequences of first (unenhanced; **C**) and third (**D**) phases. Left TZ cancer could thus be detected only on diffusion-weighted imaging.

Some limitations in the current study warrant consideration. First, in this study, MRI findings were not compared with the results of step-section tumor mapping using the whole prostate after radical prostatectomy. Some subjects diagnosed as cancer-free by systematic TRUS-guided prostate biopsy may thus actually have had prostate cancer. Second, the sample size might have been too small to compare detectability among individual methods of MRI. Third, the use of two different sequences in DCE-MRI might have influenced the tumor detectability of DCE-MRI. Fourth, in this study, prostate biopsy was per-

formed only systematically. Additional biopsy targeting the lesion with positive MRI findings might have increased the detectability of prostate cancer. Finally, because this study was designed as a retrospective investigation, subject selection might have shown sampling biases, such as postponement of prostate biopsy for various clinical reasons by patients or urologists. Such selection bias might be associated with the relatively high prevalence (70%) of biopsy-proven prostate cancer among patients with gray-zone PSA levels in this study. Further prospective investigations with larger patient populations in whom there

is a direct correlation between findings on histologic sections and corresponding MRI studies are needed to clarify the clinical value of prostate MRI in detecting tumors in patients with gray-zone PSA levels.

In conclusion, these results indicate that an MRI protocol including T2-weighted imaging, DWI, and DCE-MRI can provide clinically useful information to urologists confronting the problem of managing patients with gray-zone PSA levels. Combined T2-weighted imaging, DWI, and DCE-MRI findings appear to be potentially useful for detecting and managing prostate cancer, even if they are performed for patients with gray-zone PSA levels.

References

1. Jemal A, Siegel R, Ward E, Hao Y, Xu J, Thun MJ. Cancer statistics, 2009. *CA Cancer J Clin* 2009; 59:225–249
2. Okihara K, Shiraishi T, Ukimura O, Mizutani Y, Kawachi A, Miki T. Current trends in diagnostic and therapeutic principles for prostate cancer in Japan. *Int J Clin Oncol* 2008; 13:239–243
3. Marugame T, Mizuno S. Comparison of prostate cancer mortality in five countries: France, Italy, Japan, UK and USA from the WHO mortality database (1960–2000). *Jpn J Clin Oncol* 2005; 35: 690–691
4. Quinn M, Babb P. Patterns and trends in prostate cancer incidence, survival, prevalence and mortality. Part II. Individual countries. *BJU Int* 2002; 90:174–184
5. Nakata S, Takahashi H, Ohtake N, Takei T, Yamanaka H. Trends and characteristics in prostate cancer mortality in Japan. *Int J Urol* 2000; 7:254–257
6. Bangma CH, Kranse R, Blijenberg BG, Schroder FH. The value of screening tests in the detection of prostate cancer. Part I. Results of a retrospective evaluation of 1726 men. *Urology* 1995; 46:773–778
7. Holmberg L, Bill-Axelsson A, Helgesen F, et al. A randomized trial comparing radical prostatectomy with watchful waiting in early prostate cancer. *N Engl J Med* 2002; 347:781–789
8. Vilanova JC, Comet J, Capdevila A, et al. The value of endorectal MR imaging to predict positive biopsies in clinically intermediate-risk prostate cancer patients. *Eur Radiol* 2001; 11:229–235
9. Catalona WJ, Partin AW, Slawin KM, et al. Use of the percentage of free prostate-specific antigen to enhance differentiation of prostate cancer from benign prostatic disease: a prospective multicenter clinical trial. *JAMA* 1998; 279:1542–1547
10. Catalona WJ, Richie JP, Ahmann FR, et al. Comparison of digital rectal examination and serum prostate specific antigen in the early detection of prostate cancer: results of a multicenter clinical trial of 6,630 men. *J Urol* 1994; 151:1283–1290

11. Wilson SS, Crawford ED. Screening for prostate cancer: current recommendations. *Urol Clin North Am* 2004; 31:219–226
12. Partin AW, Kattan MW, Subong EN, et al. Combination of prostate-specific antigen, clinical stage, and Gleason score to predict pathological stage of localized prostate cancer: a multi-institutional update. *JAMA* 1997; 277:1445–1451
13. Tchertgen MB, Oesterling JE. The effect of prostatitis, urinary retention, ejaculation, and ambulation on the serum prostate-specific antigen concentration. *Urol Clin North Am* 1997; 24:283–291
14. Matlaga BR, Eskew LA, McCullough DL. Prostate biopsy: indications and technique. *J Urol* 2003; 169:12–19
15. Kumar R, Nayyar R, Kumar V, et al. Potential of magnetic resonance spectroscopic imaging in predicting absence of prostate cancer in men with serum prostate-specific antigen between 4 and 10 ng/ml: a follow-up study. *Urology* 2008; 72:859–863
16. Kumar V, Jagannathan NR, Kumar R, et al. Transrectal ultrasound-guided biopsy of prostate voxels identified as suspicious of malignancy on three-dimensional (1)H MR spectroscopic imaging in patients with abnormal digital rectal examination or raised prostate specific antigen level of 4–10 ng/ml. *NMR Biomed* 2007; 20:11–20
17. Kubota Y, Kamei S, Nakano M, Ehara H, Deguchi T, Tanaka O. The potential role of prebiopsy magnetic resonance imaging combined with prostate-specific antigen density in the detection of prostate cancer. *Int J Urol* 2008; 15:322–326
18. Kitajima K, Kaji Y, Fukabori Y, Yoshida K, Suganuma N, Sugimura K. Prostate cancer detection with 3 T MRI: comparison of diffusion-weighted imaging and dynamic contrast-enhanced MRI in combination with T2-weighted imaging. *J Magn Reson Imaging* 2010; 31:625–631
19. Tamada T, Sone T, Jo Y, et al. Prostate cancer: relationships between postbiopsy hemorrhage and tumor detectability at MR diagnosis. *Radiology* 2008; 248:531–539
20. Tanimoto A, Nakashima J, Kohno H, Shinmoto H, Kuribayashi S. Prostate cancer screening: the clinical value of diffusion-weighted imaging and dynamic MR imaging in combination with T2-weighted imaging. *J Magn Reson Imaging* 2007; 25:146–152
21. Langer DL, van der Kwast TH, Evans AJ, Trachtenberg J, Wilson BC, Haider MA. Prostate cancer detection with multi-parametric MRI: logistic regression analysis of quantitative T2, diffusion-weighted imaging, and dynamic contrast-enhanced MRI. *J Magn Reson Imaging* 2009; 30:327–334
22. Turkbey B, Pinto PA, Mani H, et al. Prostate cancer: value of multiparametric MR imaging at 3 T for detection—histopathologic correlation. *Radiology* 2010; 255:89–99
23. Lim HK, Kim JK, Kim KA, Cho KS. Prostate cancer: apparent diffusion coefficient map with T2-weighted images for detection—a multireader study. *Radiology* 2009; 250:145–151
24. Haider MA, van der Kwast TH, Tanguay J, et al. Combined T2-weighted and diffusion-weighted MRI for localization of prostate cancer. *AJR* 2007; 189:323–328
25. Kim CK, Park BK, Lee HM, Kwon GY. Value of diffusion-weighted imaging for the prediction of prostate cancer location at 3T using a phased-array coil: preliminary results. *Invest Radiol* 2007; 42:842–847
26. Takenaka A, Hara R, Hyodo Y, et al. Transperineal extended biopsy improves the clinically significant prostate cancer detection rate: a comparative study of 6 and 12 biopsy cores. *Int J Urol* 2006; 13:10–14
27. Akin O, Sala E, Moskowitz CS, et al. Transition zone prostate cancers: features, detection, localization, and staging at endorectal MR imaging. *Radiology* 2006; 239:784–792
28. Kaji Y, Kurhanewicz J, Hricak H, et al. Localizing prostate cancer in the presence of postbiopsy changes on MR images: role of proton MR spectroscopic imaging. *Radiology* 1998; 206:785–790
29. Tamada T, Sone T, Nagai K, et al. T2-weighted MR imaging of prostate cancer: multishot echo-planar imaging vs fast spin-echo imaging. *Eur Radiol* 2004; 14:318–325
30. Langer DL, van der Kwast TH, Evans AJ, et al. Intermixed normal tissue within prostate cancer: effect on MR imaging measurements of apparent diffusion coefficient and T2—sparse versus dense cancers. *Radiology* 2008; 249:900–908
31. Choi YJ, Kim JK, Kim N, Kim KW, Choi EK, Cho KS. Functional MR imaging of prostate cancer. *RadioGraphics* 2007; 27:63–75
32. Hosseinzadeh K, Schwarz SD. Endorectal diffusion-weighted imaging in prostate cancer to differentiate malignant and benign peripheral zone tissue. *J Magn Reson Imaging* 2004; 20:654–661
33. Mueller-Lisse UG, Swanson MG, Vigneron DB, Kurhanewicz J. Magnetic resonance spectroscopy in patients with locally confined prostate cancer: association of prostatic citrate and metabolic atrophy with time on hormone deprivation therapy, PSA level, and biopsy Gleason score. *Eur Radiol* 2007; 17:371–378
34. Heijmink SW, Fütterer JJ, Hambrock T, et al. Prostate cancer: body-array versus endorectal coil MR imaging at 3 T—comparison of image quality, localization, and staging performance. *Radiology* 2007; 244:184–195
35. Riches SF, Payne GS, Morgan VA, et al. MRI in the detection of prostate cancer: combined apparent diffusion coefficient, metabolite ratio, and vascular parameters. *AJR* 2009; 193:1583–1591
36. Kim JH, Kim JK, Park BW, Kim N, Cho KS. Apparent diffusion coefficient: prostate cancer versus noncancerous tissue according to anatomical region. *J Magn Reson Imaging* 2008; 28:1173–1179
37. Kim CK, Park BK, Kim B. High-b-value diffusion-weighted imaging at 3 T to detect prostate cancer: comparisons between b values of 1,000 and 2,000 s/mm². *AJR* 2010; 194:172 [web]; W33–W37
38. Tamada T, Sone T, Jo Y, et al. Apparent diffusion coefficient values in peripheral and transition zones of the prostate: comparison between normal and malignant prostatic tissues and correlation with histologic grade. *J Magn Reson Imaging* 2008; 28:720–726